NCSL INTERNATIONAL

measure

The Journal of Measurement Science

Vol. 2 No. 3 • September 2007

In This Issue:

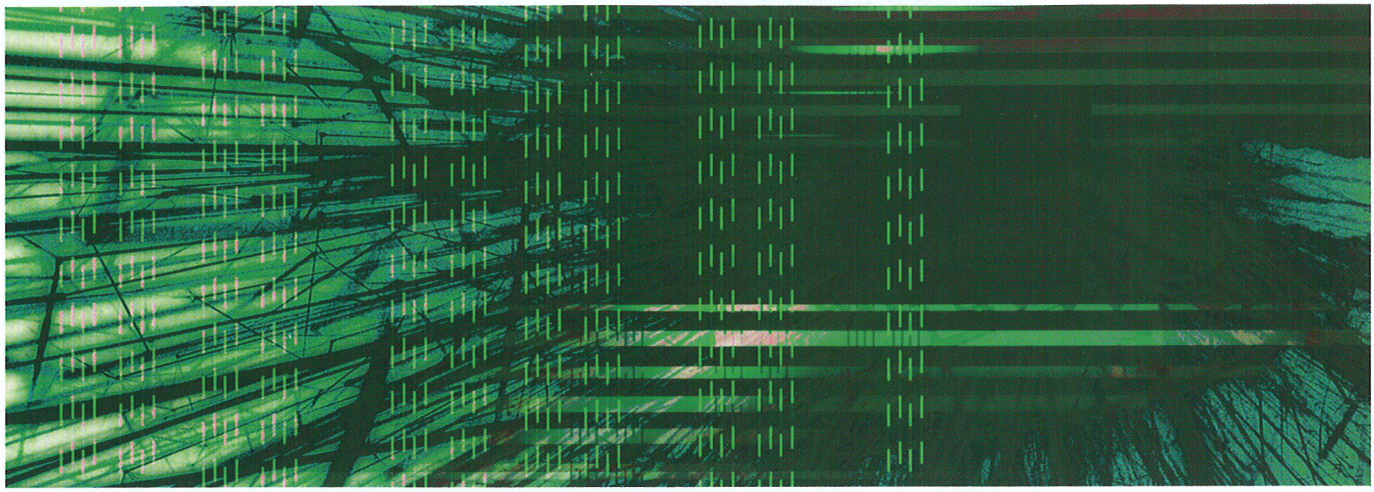

Anomalous Behavior of Teflon-based Helium Permeation Leak Standards

Patrick J. Abbott and Justin H. Chow

Abstract: Helium leak testing is a vital step in assuring product reliability for anything that must be packaged in a sealed container. Examples of problems caused by leaks abound; from leaks in blister packaging for pharmaceuticals, to leaks in aluminum wheel rims for automobiles. To quantify detected leaks, mass spectrometer-based helium leak detectors must be calibrated with one or more helium flow transfer standards, each having a quantified uncertainty. Helium permeation leak artifacts are the most popular transfer standards used for this purpose, and Teflon™ is sometimes used for the leak element in applications where mechanical shock may damage a glass element. The National Institute of Standards and Technology calibrates helium permeation leak artifacts as a function of temperature, and has found some anomalous behavior coming from Teflon -based artifacts in comparison with glass-based artifacts. These anomalies include hysteretic effects in the measured leak rate, and sudden discontinuities (jumps up or down) in the measured leak rate as a function of temperature. This behavior has been attributed to the well documented phase transitions that occur in the Teflon polymers near room temperature (19 °C and 30 °C). This paper presents data collected from commercially available Teflon -based leak standards. These data may be helpful when deciding which type of permeation transfer standard should be used to calibrate a helium leak detector for a given leak testing application.

1. Introduction

Helium leak artifacts are used to calibrate mass spectrometer-based helium leak detectors. The majority of commercially available helium leak artifacts are of the permeation type, in which a reservoir of helium at some pressure is separated from the outside world by a hollow glass frit called the leak element.

Patrick J. Abbott

Justin H. Chow

Chemical Science and Technology Laboratory
Process Measurements Division
National Institute of Standards and Technology
100 Bureau Drive; Mail Stop 8364
Gaithersburg, MD 20899 USA
Email: patrick.abbott@nist.gov

Helium readily permeates glass and, at a constant temperature, a steady-state flow through the glass develops. A diagram of a common glass element helium permeation leak artifact is shown in Fig. 1.

The flow of helium across a glass element is governed by Fick's law [1]:

$$J_N = -D\ grad N, \tag{1}$$

where J_N is the number of atoms crossing the leak element per unit area in unit time, D is the diffusivity of the leak element, and *grad N* is the gradient of the concentration of helium atoms in the glass. The diffusivity is temperature dependent and has the exponential form:

$$D = D_o\ exp\,(-E/k_BT). \tag{2}$$

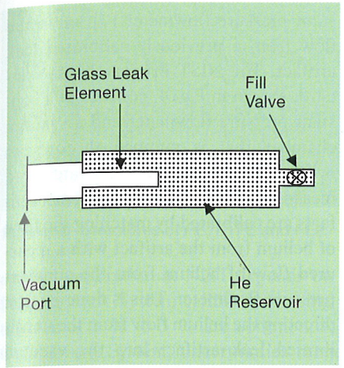

Figure 1. Glass element helium permeation leak artifact.

Here, E is the activation energy for the process, k_B is the Boltzmann constant, and T is the absolute temperature. Using equations (1) and (2), the throughput, Q, of helium permeating through the glass element of a helium permeation leak artifact (leak rate) has been given by Solomon [2] as:

$$Q = C_1 T \exp(C_2 / T), \qquad (3)$$

where C_1 is a geometrical factor that takes into account the area and thickness of the glass element and $C_2 = -E/R$, R being the molar gas constant. The constants C_1 and C_2 are determined by calibrating the leak artifact. A typical calibration curve, along with the calibration constants, is shown in Fig. 2.

The temperature dependence of the leak rate for a glass element leak artifact is typically about 3 %/°C near room temperature. After a temperature change of a few degrees, equilibrium flow is achieved in about one hour. The helium pressure in a leak artifact can be made suitably high and the reservoir volume suitably large so that even with constant flow from the artifact, the leak rate decreases by just a few percent per year. Some leak artifacts are even constructed to decay by less than 0.1 % per year. [3] Figure 3 shows a typical calibration history for a glass element helium permeation leak artifact over a 10 year time period. The decay rate is determined by the slope of the fitted line of the leak rate vs. time plot.

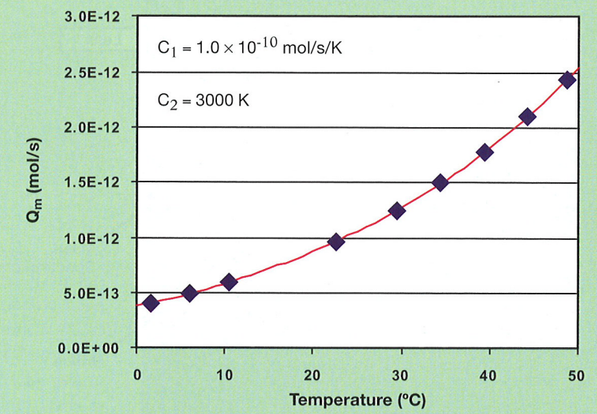

Glass Permeation Leak Artifact

Q_m = $C_1 T \exp(C_2/T)$ (mol/s)
Q_m = molar leak rate
C_1 = constant incorporating solubility, diffusivity, area and thickness of the leak element (mol/s/K)
C_2 = $-E/R$ (K)
E = diffusivity activation energy (J)
R = molar gas constant (J/mole/K)

Figure 2. Calibration data for a glass element helium permeation leak artifact.

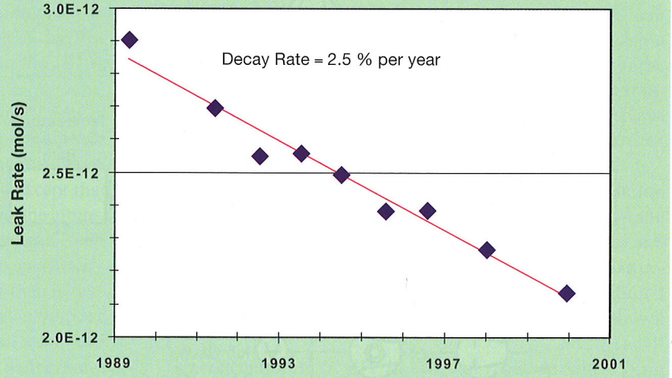

Figure 3. Calibration history for a glass element helium permeation leak artifact showing a decay rate of 2.5 % per year.

2. Calibration of Leak Artifacts

The National Institute of Standards and Technology (NIST) has operated a calibration service for permeation leak artifacts since 1987. Since then, NIST has performed over 250 helium leak calibrations for customer artifacts whose leak rates ranged from 10^{-14} to 10^{-9} moles/s (2.2×10^4 cm^3/s = 1.0 mole/s at 0 °C and 1 atmosphere pressure) [4]; many of these are repeat calibrations of the same artifact. NIST uses a comparison method to calibrate helium leak artifacts [5, 6]. The calibration of a leak artifact is performed by comparing its flow to either a flow generated and measured by a con-

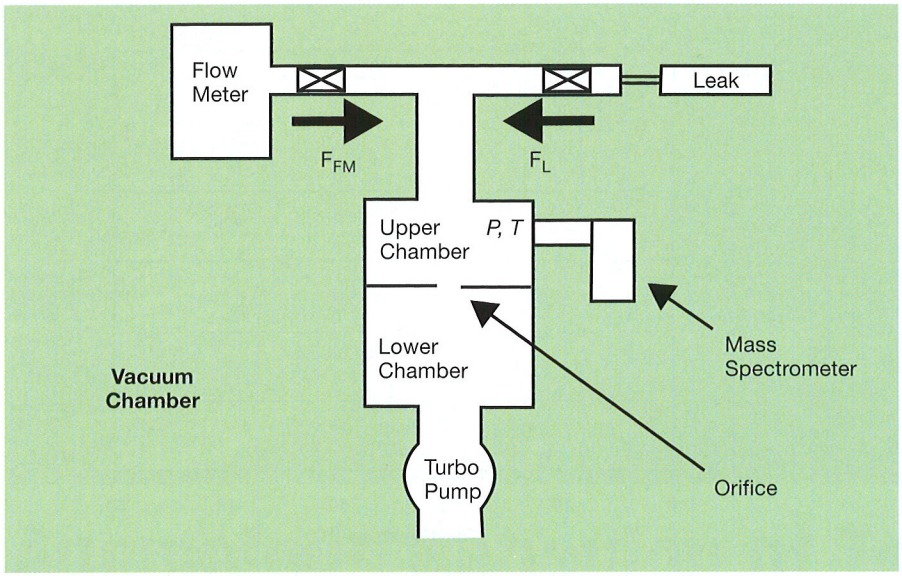

Figure 4. Schematic drawing of the NIST Primary Leak Standard, showing the major components. The partial pressure indication, P, in the uper vacuum chamber at temperature T caused by gas flow (rate F_L) from the leak is matched by flow (rate F_{FM}) from the flowmeter. The flow rate F_{FM} is then measured using the flowmeter.

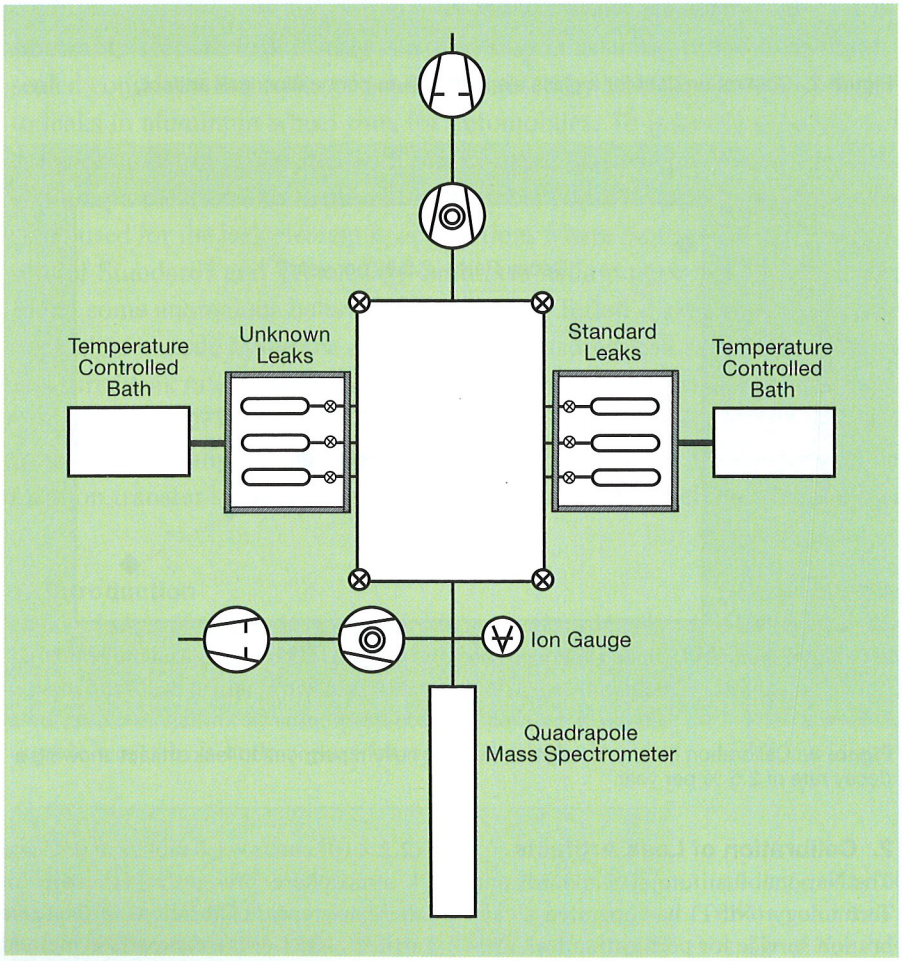

Figure 5. Schematic of the automatic NIST Leak Comparison System. The partial pressure due to flow of helium from leak artifacts to be calibrated (unknown leaks) is measured by the mass spectrometer and compared to that of transfer standards (standard leaks) as a function of the temperature of the unknown leak.

stant pressure flowmeter [7], or to the flow from a previously calibrated leak artifact. The NIST Primary Leak Standard, shown in Fig. 4, consists of a constant pressure flowmeter and a vacuum chamber that is pumped through an orifice. The flowmeter generates and measures a flow of helium gas. Leak artifacts are calibrated by matching the flow of helium from the artifact with a measured flow of helium from the constant pressure flowmeter. This is done by first directing the helium flow from the uncalibrated leak artifact into the vacuum chamber, which contains a research-grade quadrupole mass spectrometer tuned to helium, and then measuring the resulting partial pressure of helium. The flow from the leak artifact is held steady by maintaining its temperature at 23 °C ± 0.05 °C in a temperature controlled manifold. Flow from the artifact is then directed to a waste turbopump, and the partial pressure of helium in the vacuum chamber falls to its base-pressure value. Next, a flow of helium from the constant pressure flowmeter is directed into the vacuum chamber; the magnitude of this flow is adjusted so that it will generate the same partial pressure of helium in the vacuum chamber that the leak artifact did. Using this method, the flow of helium from the leak artifact is calibrated at 23 °C.

A leak artifact may also be calibrated by using another calibrated leak artifact as a transfer standard. As described above, the flow of helium from the uncalibrated leak is compared to the flow from the calibrated leak, which is maintained at a temperature of 23 °C. The automated NIST Leak Comparison System uses this technique to calibrate helium permeation leaks as a function of temperature. To do this, the flow from the uncalibrated leak is varied by setting and maintaining its temperature at several fixed values between 0 °C and 50 °C. At each temperature, the flow is compared to that of the calibrated transfer standard leak, which is maintained at 23 °C. In this way, the relationship between leak artifact temperature and flow is obtained, as shown in Fig. 2. A diagram of the automated NIST Leak Comparison System is shown in Fig. 5.

The uncertainty associated with a leak

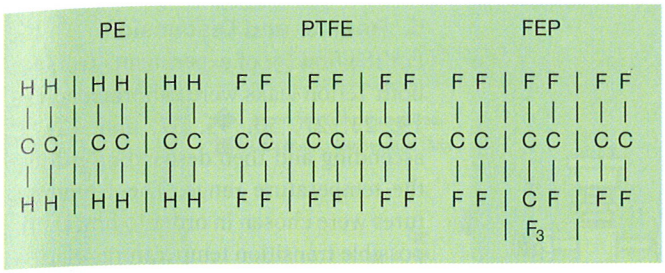

Figure 6. Structures of PE, PTFE and FEP.

artifact calibration at NIST depends on the method used: for Primary Leak System calibrations using the flowmeter, uncertainties of 1 % to 3 % are common; for the automatic Leak Comparison System, uncertainties range from about 2 % to 4 %. Both of these uncertainties are expanded to a coverage factor of $k = 2$. In general, the smaller (slower) the leak rate to be calibrated, the higher the expanded uncertainty. This is because the uncertainty of the constant pressure flowmeter increases as the desired generated flow decreases.

3. Teflon as a Leak Element

One of the major shortcomings of a glass element helium permeation leak is its fragility. If a glass permeation leak is dropped, the glass element usually shatters rendering the leak useless. To overcome this problem, manufactures have used Teflon™ as a substitute permeation element.[1] Teflon is also used as a permeation element for gases other than helium in an attempt to avoid the plugging problems that can occur with capillary leak elements. Teflon is a trademark of DuPont and is used to brand a variety of their fluoropolymers. The original Teflon fluoropolymer, polytetrafluoroethylene (PTFE), was discovered by Roy Plunkett in 1938 and was later sold commercially in the 1940's by DuPont. [8]

PTFE is known for its chemical inertness, low coefficient of friction, and wide range of operating temperatures. All of these properties are derived from PTFE's chemical structure. PTFE has the same chemical formula as polyethylene (PE) except that all of the hydrogen atoms have been replaced by fluorine atoms, as shown in Fig. 6. That is where the similarities between PTFE and PE end. Fluorine has a significantly larger electronegativity, is a larger atom, and its C-F bond strength is higher than hydrogen's C-H bond. Unlike PE, PTFE does not have a planar zigzag conformation because of fluorine's larger size. PTFE assumes a fully fluorinated, helical conformation at ambient temperature and pressure, forming chains with about 15 carbon atoms per 180° twist. [9]

These chains form an almost perfect cylinder with the fluorine atoms providing a protective outer sheath, [10], as shown in Fig. 7. This fluorine sheath gives PTFE its inertness and nonstick properties. PTFE has two phase transitions that are of particular interest because of their proximity to room temperature.

[1] Certain commercial equipment, instruments, or materials are identified in this document. Such identification does not imply recommendation or endorsement by the National Institute of Standards and Technology, nor does it imply that the products identified are necessarily the best available for the purpose.

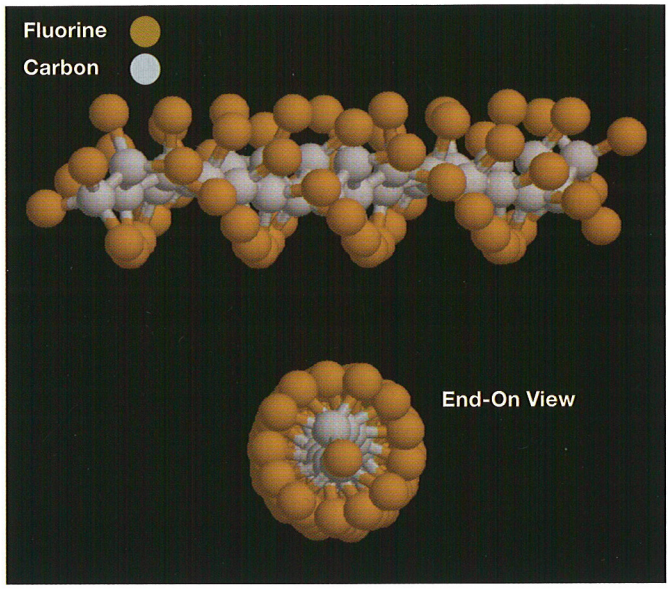

Figure 7. Structure PTFE.

Below 19 °C, the PTFE helix has a period of about 13 carbon atoms per 180° turn and has a triclinic chain-packing lattice. [10] Between 19 °C and 30 °C, the helix untwists to about 15 carbon atoms per 180° twist and has hexagonal packing. [11] A significant increase in volume (about 1 %) has been shown to accompany this phase transition. [12] Above 30 °C, the helical twisting becomes irregular and the chain packing can be described as pseudo-hexagonal. [11] An additional 0.2 % increase in original volume occurs at the 30 °C transition. According to Quinn [12] both of these transitions are reversible, but it can take more than 60 hours to establish a steady-state volume when cooling to a temperature within the transition region. However, some research has shown the transitions to be largely irreversible, as will be discussed below. Several similar fluoropolymers have since been developed, each one slightly varying the basic structure of PTFE.

The current Teflon of choice for leak manufacturers is Teflon FEP. Fluorinated Ethylene-Proplyene copolymer (FEP) is the result of the copolymerization of tetrafluoroethylene (TFE) and hexafluoropropylene (HFP). This copolymer has a similar structure to PTFE, except CF_3 groups are randomly distributed throughout the compound in place of fluorine atoms as shown in Fig. 6.

The concentration of HFP in FEP can range anywhere from almost 0 mole % to custom-made batches of 50 mol %. [13] Typical concentrations are below 15 mol %. [10] Because of its larger size than fluorine, the extra CF_3 in HFP causes an untwisting of the helix at the branch points. With increasing concentration of HFP in FEP, the two PTFE transition temperatures at 19 °C and 30 °C are lowered, eventually merging into one transition. [14] One manufacturing advantage of FEP over PTFE is that it is melt-processible. Melt processing results in a void-free fluoropolymer, meaning permeation can only occur through molecular diffusion. [8] Because PTFE is not melt-processible it can have voids and microscopic cracks throughout its structure that act like tiny capillaries. These microscopic cracks provide a second mechanism for gas permeation.

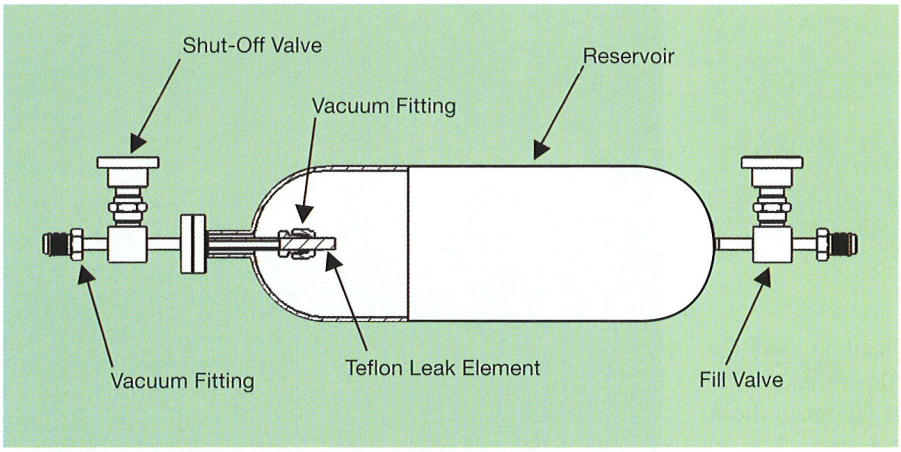

Figure 8. Schematic of a teflon permeation leak.

4. Experiments

Two commercial Teflon permeation leaks were obtained from separate manufacturers. We will refer to these leaks as *Leak A* and *Leak B*. According to the manufacturers' calibration certificates, both leaks have a leak rate of 8.5×10^{-12} mol/s at 23 °C with a temperature coefficient of 2 % / °C. *Leak A* has a fill pressure of about 300 kPa absolute (40 psia), a stated leak rate uncertainty of 12.3 % ($k = 2$), and a depletion rate of 2.3 % per year. *Leak B* has a fill pressure of 700 kPa absolute (100 psia), a stated leak rate uncertainty of 8 % ($k = 2$), and a depletion rate of 0.8 % per year. Both leaks use Teflon FEP extruded rod as a leak element; *Leak A* uses 63 mm diameter rod while *Leak B* uses 32 mm diameter rod. One design of a Teflon element permeation leak is illustrated in Fig. 8. It consists of a stainless-steel reservoir pressurized with helium, a Teflon rod leak element, some stainless-steel tubing and fittings, a fill valve, and a shut-off valve.

All of the experiments were conducted using the NIST Leak Comparison System (LCS) illustrated in Fig. 5. Up to three unknown leaks and three standard leaks can be mounted on the LCS at one time. This makes it possible to calibrate all three unknown leaks individually using one or more standard leaks. The unknown and standard leaks are mounted and a double-walled can is lowered onto each group. A temperature-controlled bath circulates ethylene-glycol anti-freeze through the walls of the can. After the leaks are mounted, they are pumped by a turbomolecular pump for 24 hours to allow their helium flows to equilibrate. The LCS is entirely automated, with the valves, temperature baths, and mass spectrometer all controlled by a computer. For customer calibrations, the unknown leaks are cycled through temperatures ranging from 0 °C to 50 °C, while the standard leaks are held at 23 °C. When changing temperatures, the computer program will set the bath temperature of the unknown leaks and then monitor a 100 Ω Platinum Resistance Thermometer (PRT) mounted on one of the leaks to determine when the set temperature has been reached. This entire process takes several hours from the time the computer sets the bath temperature to when the unknown leak is actually valved in to take data. [4, 5]

For each Teflon leak artifact, six sets of leak rate vs. temperature data were taken using the NIST Leak Comparison System. The temperatures of the artifacts were varied between 0 °C and 42 °C, though not every data set covered this entire range. It should be mentioned that the two to three hour equilibration time after a change in temperature by the LCS (as measured by platinum resistance thermometers attached to the leak artifacts under test) is far less than the 60 hour equilibration time mentioned by Quinn in reference [12]. This may account for some of the hysteresis effects seen in the data, as will be shown. For the present experiments both Teflon leaks were compared against transfer standard leak NIST 2130, which is a glass permeation leak with a leak rate of about 1×10^{-11} mol/s at 23 °C. The relative expanded uncertainty ($k = 2$) of the leak rate for NIST 2130 is 1.5 %.

5. Results and Discussion

For the first set of experiments (run #1), both Teflon leaks were calibrated at (16, 19, 23, 27, 30, 33, 37, and 42) °C, ascending and then descending through the temperature range. These temperatures were chosen in order to bracket the possible transition temperatures of 19 °C and 30 °C. Plots of the results are shown in Fig. 9. At 23 °C, *Leak A* had a leak rate of about 8×10^{-12} mol/s. Leak A behaved similarly to a glass permeation leak with the exception of the 3 % hysteresis between ascending and descending temperature data. In contrast, *Leak B* did not perform as predictably. Two large discontinuities (sudden shifts in leak rate) are evident in the results of this run. The first discontinuity occurred at 19 °C on the ascending curve and the second discontinuity occurred at 30 °C on the descending curve. These discontinuities amount to a 30 % discrepancy between the ascending and descending curves, which is *nearly four times* the manufacturer's stated uncertainty. Interestingly, the two discontinuities occur at almost the exact same temperatures as the two crystalline transitions in PTFE.

On run #2, the leaks were cycled through a very similar thermal range at temperatures of (15, 17, 19, 23, 27, 30, 35, 42) °C, ascending and descending through the temperature range. Figure 10 shows the results. There was very little change in the response of Leak A, with the hysteresis still about 3 %. However, *Leak B*'s performance changed significantly. On this run, the ascending curve follows the descending curve and then flattens out above 35 °C. The discontinuity on the ascending curve seen in run #1 has disappeared. However, the descending discontinuity remains, and follows the same curve as in run #1. This discontinuity causes a 10 % discrepancy at 35 °C between the ascending and descending curves.

Runs #1 and #2 showed a discontinuity on the descending curve between temperatures of 30 and 33 °C for *Leak B*. Therefore, on the next two runs (#3 and #4), we tried to determine more accurately the temperature of this discontinuity by limiting the temperature range to 27 to 35 °C. *Leak A* behaved as expected maintaining its 3 % hysteresis. In com-

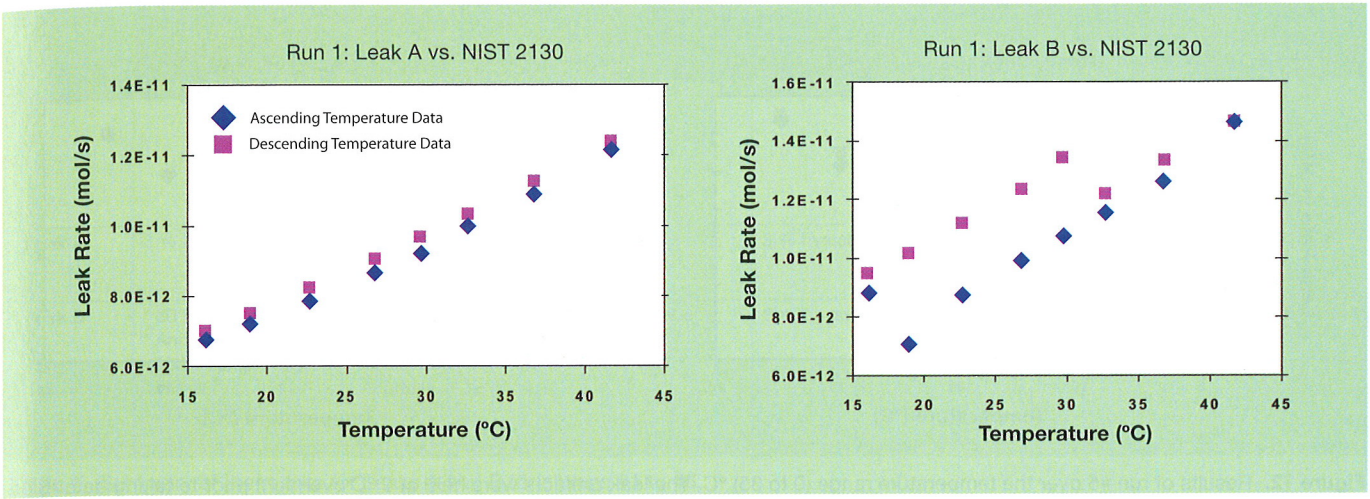

Figure 9. Results of run #1, the initial calibration run, for both leak artifacts over the range of temperatures (16 to 42) °C. Blue diamonds denote ascending and pink squares denote descending temperature data.

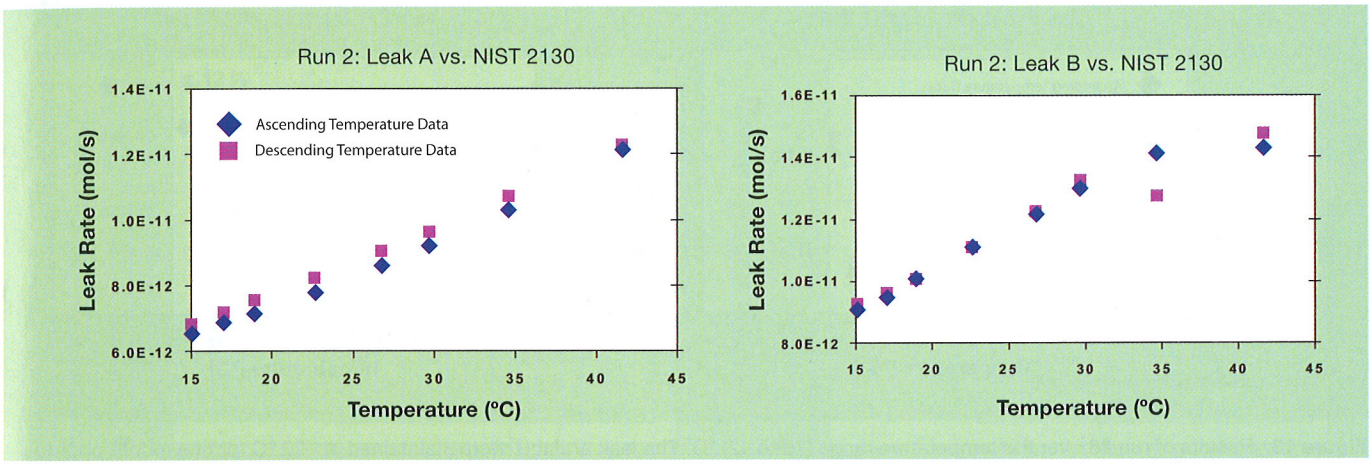

Figure 10. Results of run #2, a repeat of run #1 from (15 to 42) °C. Blue diamonds denote ascending and pink squares denote descending temperature data.

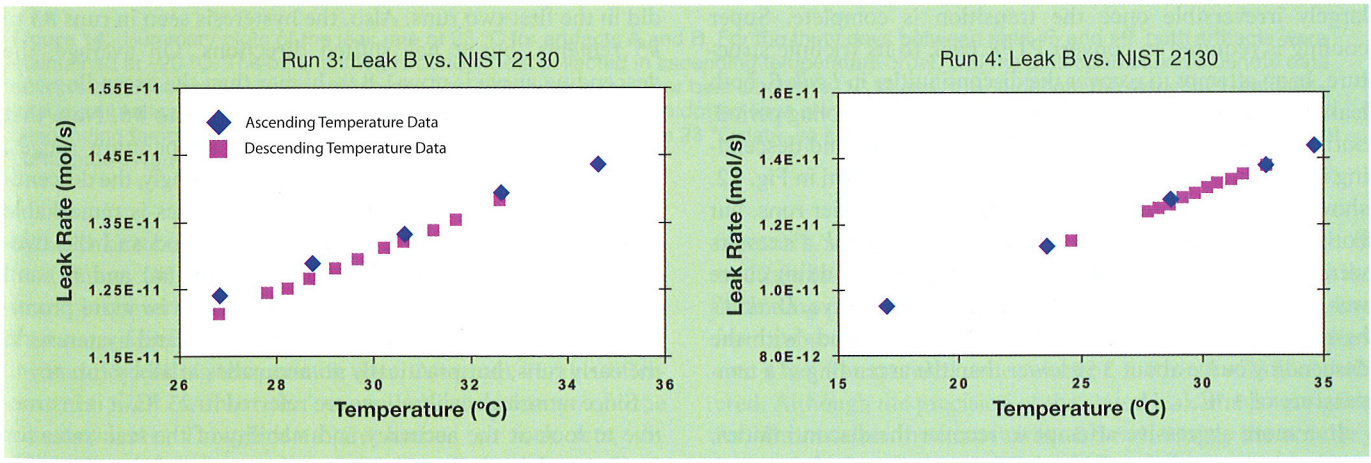

Figure 11. Results of runs #3 and #4 for *Leak B*. For run #3, the temperature range was limited to (27 to 35) °C. Run #4 included data at 0 °C. Blue diamonds denote ascending and pink squares denote descending temperature data.

parison, *Leak B* had two surprising results, as shown in Fig. 11 for runs #3 and #4. First, the discontinuity at 30 °C disappeared; second, *Leak B* exhibited hysteresis of up to a couple percent, but in a different direction than *Leak A*. For all runs, *Leak A*'s descending curve was always slightly higher than the ascending curve. However, in runs #3 and #4, *Leak B*'s descending curve was either indistinguishable from or slightly lower than the ascending curve.

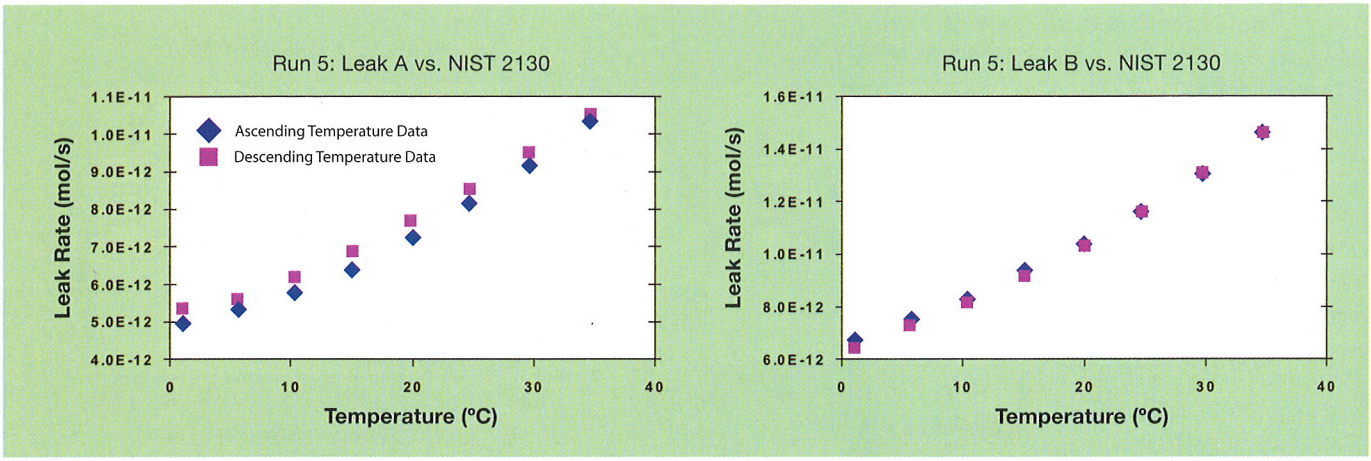

Figure 12. Results of run #5 over the temperature range (0 to 35) °C. The leak artifacts were held at 0 °C overnight prior to taking data. Blue diamonds denote ascending and pink squares denote descending temperature data.

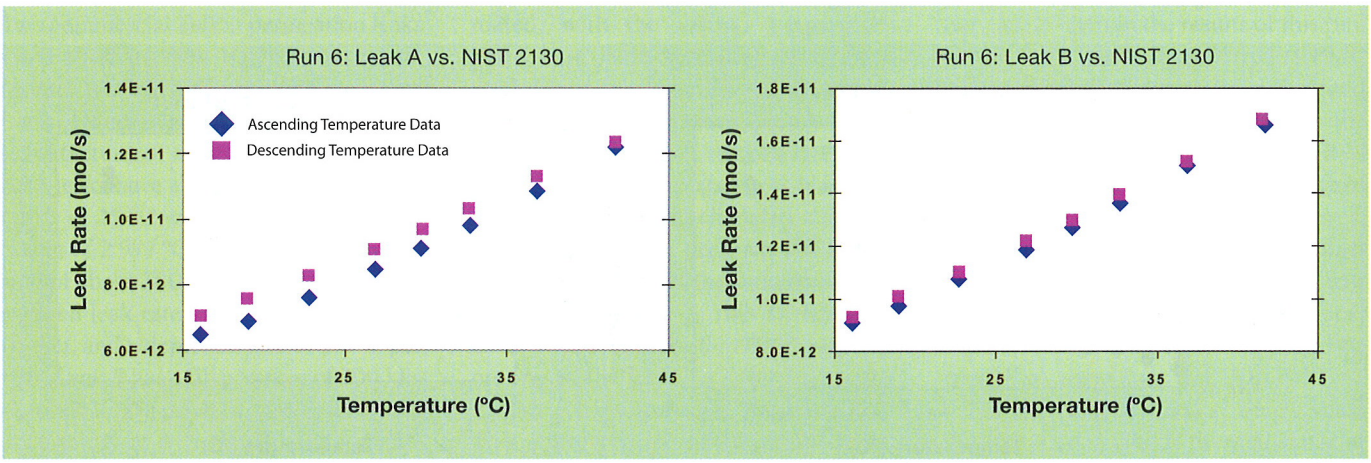

Figure 13. Results of run #6 over the temperature range (16 to 42) °C. The leak artifacts were maintained at –20 °C for one month prior to taking data. Blue Diamonds denote ascending and pink squares denote descending temperature data.

According to Androsch [15], the 19 °C transition in PTFE is largely irreversible once the transition is complete. Super cooling is required to convert PTFE back to its triclinic structure. In an attempt to recover the discontinuities in *Leak B*, both leaks were held at 0 °C overnight. Following this cooling period, both leaks were run from (0 to 35) °C ascending and descending in 5 °C increments. The results of run #5, shown in Fig. 12, showed no signs of the discontinuities seen in earlier runs, but both leaks exhibited some degree of hysteresis. *Leak A*'s results were consistent with its previous results. The descending curve was on average 4.5 % higher than the ascending curve. *Leak B*'s hysteresis was greatest at the low temperature end, with the descending curve about 3 % lower than the ascending at a temperature of 1 °C.

In a more aggressive attempt to recover the discontinuities, the leaks were taken off the LCS, put into a freezer set at –20 °C, and then left undisturbed for a month. The leaks were then mounted on the LCS and pumped for 18 hours at 23 °C in order to allow equilibration of the flow rates. A calibration run #6 was taken at the same temperatures used in run #1, and the results are shown in Fig. 13. It appears that *Leak A* has developed more severe hysteresis with an average of 5.8 % and a maximum of 8.6 % at 19 °C. *Leak B* also shows significant changes. The curves do not flatten out on the high end like they did in the first two runs. Also, the hysteresis seen in runs #3 to #5 remains, but it has shifted directions. On average, the descending curve is now 1.8 % higher than the ascending.

Table 1 summarizes the results of runs #1 to #6. Note that runs #1, #2, and #6 have very similar temperature ranges, extending from about 15 °C to 42 °C. Interestingly, the descending curves of *Leak A* are almost identical. This is remarkable given the thermal cycling the leak experienced and the two-month time frame between the first two runs (#1 and #2) and run #6. The effects of thermal cycling seem to be more prominent in *Leak B*, which exhibits discontinuities and hysteresis in the early runs, but practically no anomalies at all by run #6.

Since most leak calibrations are referred to 23 °C, it is instructive to look at the accuracy and stability of the leak rates for *Leak A* and *Leak B* at 23 °C over the course of the preceding experiments.

Figure 14 contains summary plots of this information. These plots clearly indicate the hysteresis between ascending (blue diamonds) and descending (pink squares) temperature changes on the leak rate measurements. For *Leak A*, the hysteresis is nearly constant over all runs (around 3 %), with the exception of run #6 being a little larger. Since the expanded uncertainty ($k = 2$)

	Run #1	Run #2	Run #3	Run #4	Run #5	Run #6
Notes	15 °C to 42 °C	15 °C to 42 °C	27 °C to 35 °C	17 °C to 35 °C	Leaks held at 0 °C overnight 0 °C to 35 °C	Leaks held at –20 °C for one month prior to run #6 16 °C to 42 °C
Leak A	3 % hysteresis	3 % hysteresis	3 % hysteresis	3 % hysteresis	4.5 % hysteresis	6 % hysteresis
Leak B	* 30 % hysteresis; * Anomalies at 19 °C (ascending) and 30 °C (descending)	* Nonlinear response above 35 °C (ascending); * Anomaly at 30 °C (descending)	Small hysteresis	Small hysteresis	Small hysteresis below 30 °C	2 % hysteresis below 35 °C

Table 1. Summary of the results for Leaks A and B for all runs #1 to #6.

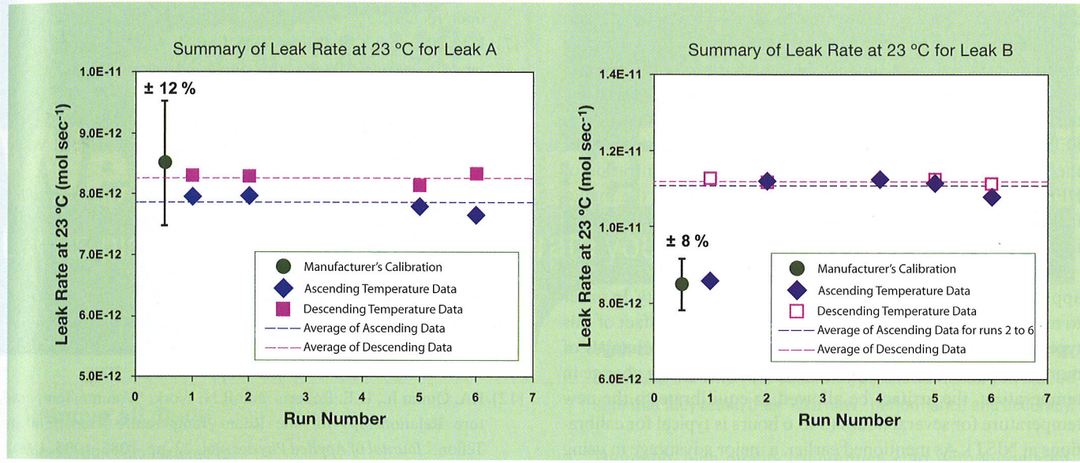

Figure 14. Summary plots of the leak rate at 23 °C for artifacts A and B. For the thirty days between runs #5 and #6, both artifacts were maintained at –20 °C. The blue diamonds denote data collected in ascending temperature order, and the pink open squares denote data collected in descending temperature order. The solid circles and error bars labeled ± 12 % and ± 8 % denote the respective manufacturer's calibration and uncertainty ($k = 2$) at the time of purchase. The dotted lines are calculated average leak rates for the ascending and descending temperature order data. Note that run #3 did not include 23 °C data, so it does not appear on the charts. Also, *Leak A* did not participate in run #4.

of the leak rate measurements is about 2 %, the uncertainty bars (not shown for clarity) from ascending and descending data would just overlap for all but run #6. For *Leak B*, only run #1 shows any significant difference in leak rate between the ascending and descending temperature data. After run #1, the difference is well within the expanded uncertainty of the measurements. Though data are limited to four sets, the descending temperature points for each artifact appear stable to well within the measurement uncertainty, as illustrated by the dotted average lines. This point is not as well illustrated with the ascending temperature data.

Regarding the accuracy of the measured leak rate, recall that the leak rate at 23 °C at the time of purchase for each artifact (as stated by the manufacturers) is 8.5×10^{-12} mol/s. As illustrated in Fig. 14, all of the data for *Leak A* overlap the manufacturer's stated value when its expanded uncertainty of ± 12 % ($k = 2$) is considered. Conversely, for *Leak B*, only the ascending point of run #1 (which is much lower than the data from subsequent runs) overlaps the manufacturer's stated leak rate when its expanded uncertainty of ± 8 % ($k = 2$) is considered. Although the precision of the stated leak rate is very good for all runs after the first (within 0.5 %), clearly the accuracy is unsatisfactory (more than 15 % from the stated value). This may indicate that the manufacturer measured the leak rate at only one temperature (about 23 °C), and that the FEP leak element had different characteristics during its NIST calibration, possibly due to a temperature-induced phase change. Thermal cycling of the artifact seems to have stabilized the temperature dependence of the leak rate for artifact B insofar as the elimination of large jumps in measured leak rate at 19 °C and 30 °C.

6. Conclusions

FEP Teflon helium permeation leaks, designated *Leak A* and *Leak B*, displayed properties that could make them undesirable as transfer standards: (1) They had a significant hysteresis (3 % to 6 %) as a function of temperature and (2) discontinuities in the measured leak rate at 19 °C and 30 °C that may be attributable to phase changes in the Teflon leak element. The hysteresis in the calibration of Leaks A and B is typical of the experiences we have had in calibrating FEP Teflon helium permeation leaks for customers. In general, customer Teflon leaks have shown hysteresis as a function of temperature that greatly exceeded the approximately 2 % uncertainty attributable to the calibration process. However, no discontinuities in the measured leak rate of the type seen in *Leak B* have been observed in customer Teflon leaks. In that regard, the data for *Leak B* suggest that thermally cycling the Teflon leak element may somehow "cure" the material and eliminate any discontinuities due to phase changes (if a curing procedure can be found, then the temperature dependence of the helium flow may become stable enough to use the artifact with increased confidence and lower uncertainty). Figure 14 illustrates the hazards of a one temperature point calibration, especially if the phase state of the FEP has not stabilized. As alluded to above, the properties of the FEP polymer may depend on the relative concentration of HFP, which is unknown to the user and possibly to the manufacturer of the leak artifact. In any case, thermal cycling seemed to help the stability of *Leak B*.

It is clear that this type of leak artifact should not be used in applications requiring the lowest leak rate uncertainty. In order to minimize the uncertainty in the leak rate of an artifact of this type, it is advised that the user avoid temperature changes of more than a few degrees C (± 3 °C), and that after a change in temperature, the artifact be allowed to equilibrate to the new temperature for several hours (3 to 6 hours is typical for calibrations at NIST). As mentioned earlier, a major advantage in using a Teflon element leak artifact is its resistance to breakage; otherwise, the cost of a glass element leak artifact is comparable with that of a Teflon element artifact, and its leak rate is much more stable and predictable.

7. Acknowledgements

It is a pleasure to acknowledge Douglas Olson and Jay Hendricks of the Pressure and Vacuum Group at NIST for many fruitful discussions during the course of this work. The authors would also like to thank Aaron Johnson and Jeanne Houston, both of NIST, for critical reviews of this manuscript and many useful suggestions.

This paper is dedicated to the memory of Dr. George Furikawa who passed away suddenly during the course of this work. Dr. Furikawa was a long-time employee of NIST, a pioneer in the measurement of the transition temperatures of Teflon, and a friend and mentor to many.

8. References

[1] Charles Kittel, *Introduction to Solid State Physics,* third edition, John Wiley & Sons, Inc., New York, 1967.

[2] G.M. Solomon, "Standardization and temperature correction of calibrated leaks," *J. Vac. Sci. Technol. A,* vol. 4, no. 3, pp. 327–333, 1986.

[3] For example, the GPP line of calibrated leak artifacts sold by Vacuum Technology Inc., 1003 Alvin Weinberg Drive, Oak Ridge, Tennessee 37830 USA.

[4] C.D. Ehrlich, "A note on flow rate and leak rate units," *J. Vac. Sci. Technol. A,* vol. 4, no. 5, pp. 2384–2385, 1986.

[5] P.J. Abbott and S.A. Tison," Commercial helium permeation leak standards: Their properties and reliability," *J. Vac. Sci. Technol. A,* vol. 14, no. 3, pp. 1242–1246, May/June 1996

[6] C.D. Ehrlich and S.A. Tison, "NIST Leak Calibration Service," *NIST Special Publication 250-38,* U.S. Government Printing Office, Washington, DC 20402-9325, January 1992. Available upon request.

[7] K.E. McCulloh, C.R. Tilford, C.D. Ehrlich, and F.G. Long, "Low-range flowmeters for use with vacuum and leak standards," *J. Vac. Sci. Technol. A,* vol. 5, no. 3, pp. 376–381, 1987.

[8] S.V. Gangal, "Perfluorinated Polymers, Polytetrafluoroethylene," in *Encyclopedia of Polymer Science and Technology,* John Wiley and Sons, Inc., vol. 3, pp. 378, 2004.

[9] S. Ebnesajjad, *Fluoroplastics Volume 1: Non-Melt Processible Fluoroplastics,* Norwich, NY Plastics Design Library, p. 10, 2000.

[10] G.P. Koo, "Structure and Mechanical Properties of Fluoropolymers," in *Fluoropolymers,* edited by L. A. Wall, Wiley-Interscience, New York, NY, p. 509, 1972.

[11] R. Androsch, B. Wunderlich, and H.-J. Radusch, "Analysis of Reversible Melting in Polytetrafluoroethylene," *Journal of Thermal Analysis and Calorimetry,* vol. 79, pp. 615–622, 2005.

[12] F.A. Quinn Jr., D.E. Roberts, and R.N. Work, "Volume-Temperature Relationships for the Room Temperature Transition in Teflon," *Journal of Applied Physics,* vol. 22, pp. 1085–1086, 1951.

[13] M.L. White, A.J. Waddon, E.D.T. Atkins, and R.J. Farris, "Copolymerization of hexafluoropropylene and tetrafluoroethylene: Effect on chain conformation and crystal structure," *Journal of Polymer Science Part B-Polymer Physics,* vol. 36, pp. 2811–2819, 1998.

[14] C. A. Rachele Pucciariello, "Phase behavior of crystalline blends of poly(tetrafluoroethylene) and of random fluorinated copolymers of tetrafluoroethylene," *Journal of Polymer Science Part B-Polymer Physics,* vol. 37, pp. 679–689, 1999.

[15] R. Androsch, "Reversibility of the low-temperature transitions of polytetrafluoroethylene as revealed by temperature- modulated differential scanning calorimetry," *Journal of Polymer Science Part B-Polymer Physics,* vol. 39, no. 7, p. 750–756, 2001.